

The race for supersymmetry: using m_{T2} for discovery

Alan J. Barr^{1,*} and Claire Gwenlan^{1,†}

¹*Denys Wilkinson Building, Keble Road, Oxford, OX1 3RH, United Kingdom*

(Dated: October 23, 2018)

We describe how one may employ a very simple event selection, using only the kinematic variable m_{T2} , to search for new particles at the LHC. The method is useful when searching for evidence of models (such as R -parity conserving supersymmetry) which have a Z_2 parity and a weakly-interacting lightest parity-odd particle. We discuss the kinematic properties which make this variable an excellent discriminant against the great majority of Standard Model backgrounds. Monte Carlo simulations suggest that this approach could be used to discover supersymmetry with somewhat smaller integrated luminosities (or perhaps lower center-of-mass energies) than would be required for other comparable analyses.

I. INTRODUCTION

The search for new particles cannot be divorced from measurement of their masses. Indeed new particles have usually been discovered by measuring differential distributions in variables sensitive to their mass [1, 2]. A notable example was the successful W boson search at the CERN Sp \bar{p} S collider [1, 3] using the transverse mass, m_T . Using the right variables can improve the discrimination between signal and background, increase the statistical power and thus expedite discovery.

One of the primary goals of the Large Hadron Collider (LHC) is to search for physics beyond the Standard Model. Many well-motivated models of new physics [4] have a Z_2 parity (for example R -parity in supersymmetry) which predicts the presence of stable, presumed weakly-interacting, particles which would contribute to the astronomical dark matter. Such particles must be produced in pairs and would be invisible to the LHC detectors.

In this paper we explain why the m_{T2} variable, which was originally proposed [5] for supersymmetric particle mass determination in hadron colliders, is also useful in *searches* for such models.¹

We start by recalling the definition of the transverse mass and its generalisation m_{T2} , and outline their defining properties (Section II). In Section III we show that experimentally-interesting kinematic configurations often lead to near-minimal values of m_{T2} . In Section IV we explain why these properties should cleanly separate new physics signals from the great majority of the Standard Model background events. A Monte Carlo simulation of a typical di-jet channel can be found in Section V. We discuss the results and conclude in Section VI.

II. DEFINITIONS

The familiar transverse mass, which was used for the W boson discovery, is defined by

$$m_T^2 \equiv m_v^2 + m_i^2 + 2(e_v e_i - \mathbf{v}_T \cdot \mathbf{q}_T), \quad (1)$$

where m_v and m_i are the masses of the visible and invisible systems respectively (e.g. the electron and neutrino for the W case), \mathbf{v}_T and \mathbf{q}_T are their momenta in the transverse plane, and the transverse energies are defined by

$$e_v^2 = m_v^2 + \mathbf{v}_T^2 \quad \text{and} \quad e_i^2 = m_i^2 + \mathbf{q}_T^2.$$

The transverse momentum \mathbf{q}_T of the unobserved neutrino can be inferred from momentum conservation in the directions perpendicular to the beam: it is assumed to be equal to the missing transverse momentum, \mathbf{p}_T which is defined to be the negative sum of the transverse momenta of all the particles observed in the detector (i.e. including hadrons in the W case).

Why was m_T useful for the W search? The defining property of m_T is as follows: for events in which a visible and an invisible system originate from the decay of a single parent particle of mass m_0 , and when the correct daughter masses are used, m_T satisfies

$$m_T \leq m_0 \quad (2)$$

by construction², with equality when the rapidity of all invisible daughters is equal to that of the visible system. The transverse mass gives the lowest event-by-event upper bound on m_0 . The maximum value of m_T over all events therefore delineates the boundary between allowed and forbidden values of the parent mass, m_0 .

For the W boson search the allowed values of m_T could therefore span a range $m_{<} \lesssim m_T \lesssim m_W$ for signal events. The lower bound is given by $m_{<} = m_v + m_i$, which is zero if one assumes (as was done implicitly in

*Electronic address: a.barr@physics.ox.ac.uk

†Electronic address: c.gwenlan@physics.ox.ac.uk

¹ Some of these observations were originally made in a talk at CERN by the authors in May 2007. Since then, the method has been employed, for example in [6], but the underlying properties which represented the motivation for the approach have not previously been published.

² If the width of the particle and the experimental resolutions are assumed to be small.

the original W search papers) that both m_ν and m_i are zero. Other processes which could have led to lepton + \mathbf{p}_T final states, for example leptonic decays of τ leptons or B hadrons were also constrained by similar inequalities, but these backgrounds have smaller values of m_0 . There was therefore a region bounded approximately by $m_B \lesssim m_T \lesssim m_W$ in which there were very few background events and a preponderance of the signal.³

A corresponding construction can be made for the types of LHC search described in the introduction. We are now interested in the case in which *two* new particles are produced, each of which decays to a set of (one or more) visible and (one or more) invisible daughters. We label the two branches of the decay with the superscripts (1) and (2) to distinguish them, and for the purposes of this paper assume that the visible particles can be unambiguously assigned to one or other parent, though this need not be done in general [7]. According to our assumptions, each invisible system should include one dark matter candidate.

As was the case for single-particle decays, there will be some values of parent and (visible and invisible) daughter masses which are consistent with the observed momenta, and others which are not.

The \mathbf{p}_T constraint needs some modification compared to the single decay case. For a pair of invisible systems the transverse momentum of each the two invisible-particle systems is not individually known, but the sum is constrained by $\mathbf{q}_T^{(1)} + \mathbf{q}_T^{(2)} = \mathbf{p}_T$. One can construct the boundary between the allowed and disallowed regions using the variable m_{T2} [5]

$$m_{T2}(v_1, v_2, \mathbf{p}_T, m_i^{(1)}, m_i^{(2)}) \equiv \min_{\sum \mathbf{q}_T = \mathbf{p}_T} \left\{ \max(m_T^{(1)}, m_T^{(2)}) \right\}. \quad (3)$$

For decays of two parents, each of mass m_0 , m_{T2} gives the lowest upper bound on m_0 consistent with the observed momenta and the hypothesised daughter masses. The maximum of m_{T2} over events therefore delineates the boundary of the domain (in the space of parent and daughter masses) which is consistent with the observed momenta [8]. It is this bounding property which makes it ideally suited for measuring supersymmetric particle masses at the LHC [7, 8, 9, 10, 11]. It has also recently been used to measure the top quark mass at the Tevatron [12].

We note that the Lorentz 2+1 dimensional vectors $v = (e_\nu, \mathbf{v}_T)$ and $i = (e_i, \mathbf{q}_T)$ can each represent single particles or multi-body systems. For example v could represent an individual lepton, or a jet or a di-jet pair. Similarly each of the invisible-particle systems may represent a single massive invisible particle (such as a $\tilde{\chi}_1^0$) or a single particle of negligible mass (neutrino) or a set of

invisible particles (e.g. $\tilde{\chi}_1^0 + \nu$). For composite systems, the composite 2+1 vectors can be formed from the vector sum of the 2+1 vectors of their individual constituents.⁴

III. RELEVANT PROPERTIES

Later in Section IV and V, we shall find that many background processes predict values of m_{T2} near the global minimum, $m_<$. The value of this minimum is therefore of some interest. It follows from (3) that

$$m_< = \max(m_<^{(1)}, m_<^{(2)}), \quad (4)$$

where $m_<^{(n)} = m_\nu^{(n)} + m_i^{(n)}$ is the global minimum of each of the two individual $m_T^{(n)}$.

In order to construct m_{T2} we require hypotheses for the invisible particle(s) masses $m_i^{(n)}$. In a search we usually don't know *a priori* whether any invisible particles are massive (or if so, what those masses are) so we choose to set the invisible-particle mass hypotheses m_i to zero. This is the only value guaranteed to preserve (2) if the invisible particles' true masses are unknown.⁵ It is also the appropriate choice for background processes where the invisible particles are (\sim massless) neutrinos.

In the rest of this section we show that the observable $m_{T2}(v_1, v_2, \mathbf{p}_T, 0, 0)$ must adopt small values for a variety of kinematic configurations. In Section IV we use these results to show that such configurations are satisfied (at least approximately) by very many of the Standard Model processes which represent backgrounds to example searches.

Lemma 1 *When a pair of particles are produced, both with mass m_0 , and each parent decays to a visible system v and an invisible system i , then $m_{T2}(v_1, v_2, \mathbf{p}_T, 0, 0) \leq m_0$.*

Proof Consider the chained pair of inequalities $m_{T2}(v_1, v_2, \mathbf{p}_T, 0, 0) \leq m_{T2}(v_1, v_2, \mathbf{p}_T, m_i^{(1)}, m_i^{(2)}) \leq m_0$. The first inequality follows since each $m_T^{(n)}$ is a monotonic function of the (non-negative) parameter $m_i^{(n)}$. The second inequality is satisfied by m_{T2} by construction: one of the partitions of the missing momentum is the correct one, and for that partition each $m_T \leq m_0$ by (2).

Lemma 2 *When two particles are produced with different masses m_1 and m_2 and each parent decays to a visible system v and an invisible system i then $m_{T2}(v_1, v_2, \mathbf{p}_T, 0, 0) \leq \max(m_1, m_2)$.*

³ In [1] the lower end of this distribution was removed because of threshold cuts on the electron p_T and \cancel{p} .

⁴ Alternative combinatorial procedures are available for the *visible* system [13].

⁵ If and when signals suggesting new invisible particles are observed, their masses can later be determined, for example by constructing variables sensitive to the kink in the maximum of m_{T2} is as a function of the input value of m_i [9, 10].

Proof As for Lemma 1 except that at the correct \mathbf{p}_T partition we can only be sure that $m_T^{(1)} \leq m_1$ and $m_T^{(2)} \leq m_2$ and so $\max(m_T^{(1)}, m_T^{(2)}) \leq \max(m_1, m_2)$ for that partition.

Lemma 3 When $\mathbf{v}_T^{(n)} = \mathbf{0}$ and $m_v^{(n)} = m_i^{(\bar{n})} = 0$ then $m_{T2} = m_{<}$; for $n \in \{1, 2\}$.

Proof Without loss in generality let $n = 2$ (and so $\bar{n} = 1$). Now $m_T^{(2)} = m_{<}^{(2)} \vee \mathbf{q}_T^{(2)}$. There exists a partition of \mathbf{p}_T with $\mathbf{q}_T^{(1)} = \mathbf{0}$ for which $m_T^{(1)} = m_{<}^{(1)}$. The result follows from (3) and (4).

An important example of Lemma 3 is the decay of a single parent of mass m_0 . The second (non-existent) visible system is represented by $v_2 = (0, \mathbf{0})$. With $m_i^{(1)} = 0$, Lemma 3 shows that $m_{T2} = m_{<} = \max(m_i^{(2)}, m_v^{(1)})$ where the second equality is a result of (4).

Lemma 4 When $\mathbf{p}_T = \mathbf{0}$ and $m_i^{(1,2)} = 0$ then $m_{T2} = m_{<}$.

Proof For $\mathbf{p}_T = \mathbf{0}$ there exists a trivial partition of the missing momentum with $\mathbf{q}_T^{(1)} = \mathbf{q}_T^{(2)} = \mathbf{0}$. For that partition, $m_T^{(1)} = m_{<}^{(1)}$ and $m_T^{(2)} = m_{<}^{(2)}$; the result follows from (3) and (4).

Lemma 5 When $m_i^{(1,2)} = 0$, $m_v^{(n)} = 0$ and $\mathbf{p}_T \parallel \mathbf{v}_T^{(n)}$ then $m_{T2} = m_{<}$; for $n \in \{1, 2\}$.

Proof Without loss of generality let $n = 1$. There exists a partition of \mathbf{p}_T with $\mathbf{q}_T^{(1)} = \mathbf{p}_T$ and $\mathbf{q}_T^{(2)} = \mathbf{0}$. Each m_T is equal to its global minimum by (1), and the result follows from (4).

Lemma 6 When $m_i^{(1,2)} = m_v^{(1,2)} = 0$, and \mathbf{p}_T can be expressed as the sum $\mathbf{p}_T = \sum_k x_k \mathbf{q}_T^k$ for some real non-negative x_k then $m_{T2} = m_{<} = 0$.

Proof For the partition of \mathbf{p}_T given by these x_k , $\mathbf{q}_T^{(n)} \parallel \mathbf{v}_T^{(n)}$ simultaneously for both $n \in \{1, 2\}$. For that partition each $m_T^{(n)} = m_{<}^{(n)} = 0$. The result follows from (3) and (4).

Lemma 7 If either or both visible systems are composite, then each of the results in Lemmas 1 – 6 also hold when either or both the composite Lorentz 2+1 vectors v are replaced by any subset of their (respective) constituents.

Proof Lemmas 3 – 6 follow exactly as before. For Lemmas 1 and 2 it is sufficient to show that m_{T2} cannot be increased when a constituent is removed from a composite (visible) system.

Now m_T^2 is the inner product of a sum of Lorentz 2+1 vectors

$$m_T^2 = (v + i)^2 = \left(\sum c_k \right)^2,$$

where the sum runs over all the constituent c_k , whether visible or invisible. Separating one of the visible particles, c_j and letting $\sigma = \sum_{k \neq j} c_k$,

$$m_T^2 = \sigma^2 + v_j^2 + 2\sigma \cdot v_j.$$

Since each of the constituent vectors is time-like (or null) each of the terms is non-negative and $\sigma^2 \leq m_T^2$. But $\sqrt{\sigma^2}$ is precisely the transverse mass one obtains if v_j is omitted, so the transverse mass cannot be increased by omitting a particle. This result also holds at the partition chosen by the minimisation of (3) so m_{T2} is never increased by omitting one (or by induction more than one) of the visible particles.

Physically relevant configurations will rarely (if ever) conform to the precise configurations described in Lemmas 1 – 7; parent particles will be off-mass-shell, Standard Model particles will have small but non-zero masses, \mathbf{p}_T will never be exactly zero nor vectors exactly parallel. However, since m_T is a continuous function of its inputs, kinematic configurations close to those described above will have upper bounds close to these idealised cases.

IV. EXAMPLE

The properties described in Section III turn out to be particularly useful for various LHC searches. We demonstrate the reasons why by examining the concrete example of pair-production of heavy, strongly-interacting particles of mass m_0 , each of which decays to a light-quark jet and an invisible particle. The characteristic final state is thus two (usually high- p_T) jets with significant \mathbf{p}_T . Examples of models which could lead to such a final state can be found in Table I.

Supersymmetry :	$\tilde{q} \bar{\tilde{q}} \rightarrow q \tilde{\chi}_1^0 \bar{q} \tilde{\chi}_1^0$
UED :	$q_1 \bar{q}_1 \rightarrow q \gamma_1 \bar{q} \gamma_1$
Leptoquarks :	$LQ \overline{LQ} \rightarrow \nu \bar{\nu} \bar{\nu} \nu$

TABLE I: Examples of models of new physics producing di-jets in association with \mathbf{p}_T .

When considering how to search in such channels, a variety of levels of sophistication can be envisioned.

In a typical cut-based search one would select events with large \mathbf{p}_T and two high- p_T jets; require sufficiently large azimuthal angles $\Delta\phi_j$ between each jet and the \mathbf{p}_T vector to reduce backgrounds from “fake” (from the mis-measurement of one of the jet energies) or “real” (from neutrinos in jets) \cancel{p} from the jet; and apply further cuts to reduce background processes (such as leptonic $t\bar{t}$ decays) which produce neutrinos and high- p_T jets with larger $\Delta\phi_j$ [6]. The remaining events should be signal-enriched, and so, provided that the residual background contributions can be understood, one can check for an excess of events not explained by the Standard Model. The

Process	$m_{T2}(v_1, v_2, \not{p}_T, 0, 0)$	Comments
QCD di-jet \rightarrow hadrons	$= \max m_j$ by Lemmas 1,4	
QCD multi jets \rightarrow hadrons	$= \max m_j$ by Lemma 4	
$t\bar{t}$ production	$= \max m_j$ by Lemma 4	fully hadronic decays
	$\leq m_t$ by Lemmas 1,7	any leptonic decays
Single top / tW	$= \max m_j$ by Lemma 4	fully hadronic decays
	$\leq m_t$ by Lemmas 2,7	any leptonic decays
Multi jets: “fake” \not{p}_T	$= \max m_j$ by Lemma 5	single mismeasured jet ^a
	$= \max m_j$ by Lemma 6	two mismeasured jets ^a
Multi jets: “real” \not{p}_T	$= \max m_j$ by Lemma 5	single jet with leptonic b decay ^a
	$= \max m_j$ by Lemma 6	two jets with leptonic b decays ^a
$Z \rightarrow \nu\bar{\nu}$	$= 0$ by Lemma 3	
$Zj \rightarrow \nu\bar{\nu}j$	$= m_j$ by Lemma 3	one ISR jet ^a
$W \rightarrow \ell\nu$ ^b	$= m_\ell$ by Lemma 3	
$Wj \rightarrow \ell\nu j$ ^b	$\leq m_W$ by Lemma 2	one ISR jet ^a
$WW \rightarrow \ell\nu\ell\nu$ ^b	$\leq m_W$ by Lemma 1	
$ZZ \rightarrow \nu\bar{\nu}\nu\bar{\nu}$	$= 0$ by Lemma 3	also $= m_j$ for one ISR jet ^a
$LQ\bar{L}\bar{Q} \rightarrow q\nu\bar{q}\bar{\nu}$	$\leq m_{LQ}$	} i.e. can take large values
$\bar{q}\bar{q} \rightarrow q\bar{\chi}_1^0\bar{q}\bar{\chi}_1^0$	$\leq m_{\bar{q}}$	
$q_1, \bar{q}_1 \rightarrow q\gamma_1, \bar{q}\gamma_1$	$\leq m_{q_1}$	

^a Assuming that the relevant jet(s) are identified with one of the two visible particle systems $v^{(n)}$.

^b Even if the lepton is mistaken for a jet.

TABLE II: Examples of Standard Model backgrounds, various signals, and associated values of m_{T2} . In the cases marked ^b, there are more restrictive upper bounds if the lepton is assumed not to be misidentified as a jet.

most difficult task is to understand the contribution of the background to the selected events – for which a variety of techniques have been proposed [6, 14]. Applying such a set of many single-variable cuts is fairly straightforward but is somewhat wasteful of signal events (which one can assume will be in scarce supply at the time of any interesting discovery).

At the other extreme, the formally optimal search method (needing the fewest events) would require calculation of the likelihood for all events for every signal and background hypothesis. This is often prohibitively difficult in practice even if all such hypotheses can be identified and modelled.

A pragmatic approach, intermediate in complexity, is to find a single, easily-calculable observable which, while not optimal in the formal statistical sense, still gives very good discrimination between the majority of signal-like and background-like events, based on some rather general principles such as relativistic kinematics. In what follows we shall find that m_{T2} is just such an observable.

For the example search channels, we identify the two visible systems $v^{(n)}$ with the two highest- p_T jets. Our jets, though massive, should have a sufficiently small mass that $m_j \approx 0$ is a good approximation. For the reasons discussed in Section III we set both $m_i^{(n)}$ to zero. For these choices, $m_{<}$ is small (equal to the larger of the $m_j^{(n)}$) and the mass conditions required for Lemmas 3 – 7 are satisfied in the $m_j \rightarrow 0$ limit.

Table II lists a variety of Standard Model processes which form backgrounds to the search channel. From Lemmas 1 – 7 we expect to find restrictive upper bounds on m_{T2} for many of these. Processes with small \not{p}_T ; with small jet p_T ; with small $\Delta\phi_j$; or from production of one or two Standard Model particles; all bound m_{T2} from above. Such processes constitute the majority of both the “physics” and “detector” backgrounds to this channel so one can remove the vast majority of the background simply by requiring large m_{T2} . No additional cuts are required – other than perhaps modest trigger requirements on jet p_T or on \not{p}_T .

An example “physics” background is $t\bar{t}$ production. This is pair-production of equal-mass particles, so m_{T2} is bounded above by the mass of the top quark m_t by Lemma 1. One could argue that this is not a very strict bound, but it is much smaller than masses of the particles typically being searched for, and the top is the heaviest known Standard Model particle, so other similar background processes, e.g. hadronic $\tau^+\tau^-$ decays should adopt smaller values of m_{T2} again.

An example of a detector-induced background is “fake” \not{p}_T – events with no invisible particles, but where a substantial fraction of the energy of one of the leading jets is lost. This can happen when energy is deposited in inactive material the detector (e.g. cables, services or support structures). Such pathological events cannot necessarily be cleanly identified. In these cases the detector usu-

ally measures a jet with Lorentz 2+1 vector $j' = \alpha j$ ($0 < \alpha < 1$), and one gains a contribution to \cancel{p}_T of $(\alpha - 1)\mathbf{j}_T$. In the absence of any other source of missing momentum, $\cancel{p}_T \parallel \mathbf{j}_T$, so $m_{T2} \rightarrow m_<$ by Lemma 5 or 6. Similar arguments apply to heavy-quark jets where leptonic decays lead to production of neutrinos close to the jet axis.

The other backgrounds in Table II are also forced to small values of m_{T2} . The least restrictive is $\leq m_t$ since the top is (assumed here to be) the heaviest Standard Model particle.

What values of m_{T2} are expected for any new particles? At the upper end it is clear from Lemma 1, that $m_{T2} \leq m_0$ for the processes in Table II. One needs a significant number of events with $m_{T2} > m_t$ to have a signal region which is relatively free of background. Now if the correct value of m_i were to be used then the upper bound (m_0) would be saturated since there is a significant density of states with $m_{T2}(v_1, v_2, \cancel{p}_T, m_i, m_i)$ close to m_0 . We have chosen to input the lowest conceivable value $m_i \rightarrow 0$ rather than the true invisible-particle mass, so the argument does not prove that the bound is saturated. However one can see from (1) that, provided $m_i \ll |\mathbf{q}_T|$, then events which are close to maximal when the true m_i is used will also remain close when we replace this by $m_i = 0$.

We therefore expect to find a large number of signal events, and very little background, in the region approximately bounded by $m_t \lesssim m_{T2} \lesssim m_0$, where m_0 is the mass of the new particle.

V. SIMULATION

To illustrate the results of Section III and Section IV we generate Monte Carlo signal and background samples with Herwig++ 2.3.2 [15]. The background processes simulated are QCD, $t\bar{t}$, $W \rightarrow \ell\nu + \text{jets}$, $Z \rightarrow \ell^+\ell^- + \text{jets}$, and $Z \rightarrow \nu\bar{\nu} + \text{jets}$. The contribution from diboson+jets is expected to be very small [6] so is not considered here. In order to generate sufficient QCD events in the high- p_T region, eight samples were generated in slices of the p_T of the hard scatter. For the SUSY signal, the SPS1a point [16] is used ($m_0 = 100$ GeV, $m_{1/2} = 250$ GeV, $A_0 = -100$ GeV, $\tan\beta = 10$, $\mu > 0$), as calculated by SPheno 2.2.3 [17]. Table III lists the leading order cross sections calculated by Herwig++, and the number of events generated for each of the processes considered.

We cluster hadrons (and π^0 s) with fiducial pseudorapidity ($|\eta| < 5$) and momentum ($p_T > 0.5$ GeV) into jets using the fastjet [18] implementation of the anti- k_T algorithm [19]. We use the E combination scheme and set $R = 0.4$ and $p_T^{\text{min}} = 10$ GeV. To simulate the detector effects we smear the majority ($1 - \epsilon$) of the jet energies

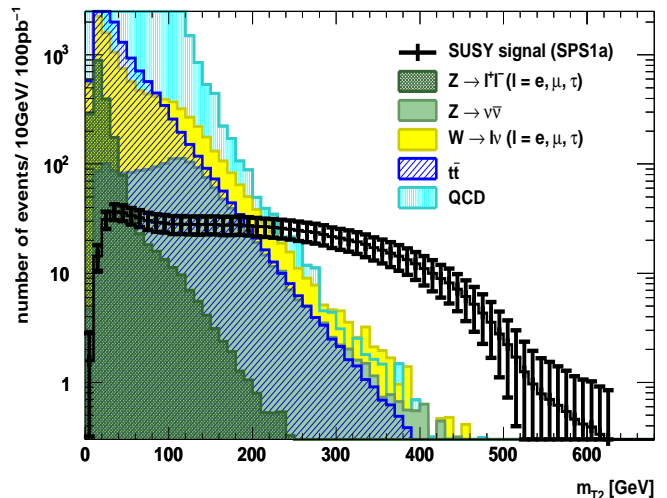


FIG. 1: Distribution of m_{T2} for events with two or more jets with $p_T > 50$ GeV (and no other cuts). For the signal point the squark masses are in the range $500 \lesssim m_{\tilde{q}} \lesssim 600$ GeV and the gluino mass is close to 600 GeV.

by a Gaussian probability density function of width

$$\sigma(E)/E_j = \left(0.6/\sqrt{E_j[\text{GeV}]}\right) \oplus 0.03$$

where E_j is the unsmeared jet energy. This resolution is typical of one of the general-purpose LHC detectors [6, 14]. Since the tails of the \cancel{p}_T distribution are often dominated by badly mismeasured jets, we simulate pathological energy-loss by applying a different smearing function to the remaining fraction ($\epsilon = 0.1\%$) of the jets⁶ with probability density:

$$P(E) = \begin{cases} 2E/E_j^2 & \text{for } (0 < E < E_j) \\ 0 & \text{elsewhere} \end{cases}$$

The missing transverse momentum is calculated from the negative vector sum of the visible fiducial hadrons (including π^0) and is corrected for the jet smearing. We impose the simple requirement that each event contains at least two jets with $p_T > 50$ GeV. We then take the two highest p_T jets as $j_{1,2}$ and calculate $m_{T2}(j_1, j_2, \cancel{p}_T, 0, 0)$, for all events. We normalise to 100 pb^{-1} (using the leading order cross sections for both signal and background). The resulting distribution can be seen in Figure 1.

⁶ [6] suggests a larger value of $\epsilon \sim 1\%$. We find a smaller value better matches the tails of the \cancel{p}_T and m_{T2} distributions found in full simulation. The detailed form of the transfer function clearly needs to be determined from the collision data, but our findings are not materially altered by changing epsilon from 0.1% to 1%.

sample	LO cross section (pb)	number of events
QCD ($17 < p_T < 35$ GeV)	9.44×10^8	6×10^7
QCD ($35 < p_T < 70$ GeV)	5.99×10^7	5×10^7
QCD ($70 < p_T < 140$ GeV)	3.45×10^6	5×10^7
QCD ($140 < p_T < 280$ GeV)	1.57×10^5	5×10^7
QCD ($280 < p_T < 560$ GeV)	5280	4×10^7
QCD ($560 < p_T < 1120$ GeV)	116	3×10^7
QCD ($1120 < p_T < 2240$ GeV)	1.11	2×10^7
QCD ($p_T > 2240$ GeV)	1.15×10^{-3}	5×10^6
$t\bar{t}$	231	2×10^7
$W \rightarrow \ell\nu + \text{jets}$	17,100	1.5×10^8
$Z \rightarrow \ell^\pm \ell^\mp + \text{jets}$	1780	9×10^7
$Z \rightarrow \nu\nu + \text{jets}$	3440	5×10^7
SUSY signal (SPS1a)	13.5	2×10^6

TABLE III: Signal and background processes together with their leading order cross-sections, and number of events generated for each.

As predicted, the region $m_t \lesssim m_{T_2} \lesssim m_{\tilde{q}}$ is dominated by signal events. The great majority of the Standard Model background events are found at small m_{T_2} , as required by the arguments of Section IV. The remaining backgrounds for which m_{T_2} is not bounded above by the arguments in Section IV are: $Z \rightarrow \nu\bar{\nu}$ in association with two hard jets from initial state radiation (ISR); $W \rightarrow \text{leptons plus two hard ISR jets}$; and three- (or more-) jet production where one of the jets loses a very large amount of energy, and that jet is not one of the two highest p_T jets input to m_{T_2} . For the signal point examined, and with the level of sophistication used for our simulations, we find that the residual backgrounds for $m_{T_2} \gtrsim m_t$ are well below the supersymmetric signal predictions.

VI. DISCUSSION

The numerical simulations of Section V confirm the analytic results of Section III; m_{T_2} adopts small values – equal to or less than the mass of Standard Model particles – for the vast majority of events from the background processes. The region $m_{T_2} \gtrsim m_t$ is signal-dominated; for SPS1a a single cut requiring $m_{T_2} > 230$ GeV results in a statistical significance $S/\sqrt{S+B}$ of 15, for 100 pb^{-1} of integrated luminosity at $\sqrt{S} = 10$ TeV. This is a higher significance than is found when applying to the same simulated events the selections of comparable multi-cut-based analyses e.g. [6, 20, 21].

Applying a single-variable kinematic selection based solely on m_{T_2} would be sufficient to separate the signal from the background. In practice m_{T_2} is unlikely to be calculated by the trigger algorithms (certainly not at the first level) so some thresholds for the jet p_T s and the \cancel{p}_T will be required in order to keep trigger rates within the available bandwidth, particularly at higher instantaneous luminosities. Our simulations show that adding typical

trigger requirements has the effect of removing events at small m_{T_2} (as would be expected from Lemmas 3,4). Reasonable thresholds leave the large m_{T_2} region – and hence the statistical significance – practically unchanged. The lower m_{T_2} end of the distribution can be recovered using lower-threshold prescaled triggers, so it can be used as a control region.

The remaining backgrounds at large m_{T_2} are dominated by states originating from more than two (massive or high- p_T) Standard Model particles (e.g. Zjj , Wjj , $t\bar{t}j$, jjj). The bounds of Section III do not apply to these since the variable m_{T_2} was developed for the explicit two-parent case. To reduce the residual contribution from these $n > 2$ -particle topologies one might consider using, rather than m_{T_2} , an n -parent generalisation of the transverse mass:

$$m_{T_n} \equiv \min_{\sum \mathbf{q}_T = \cancel{p}_T} \{ \max m_T^{(i)} \} \quad \text{with } i \in \{1, \dots, n\}. \quad (5)$$

Using (5) n -body background topologies (and also $m < n$ -body topologies by a generalisation of Lemma 2) would be bounded from above by the mass of the heaviest parent. The problem would be that one would no longer expect pair-produced signal topologies (such as those in Table I) to obtain m_{T_n} values close to the mass of the new heavy parent. Indeed a generalisation of Lemma 3 shows that for the simplest Z_2 signal case, di-jet + \cancel{p}_T , m_{T_3} is forced towards the small value ($\max m_j$) so one loses the discrimination power of m_{T_2} . Such $n > 2$ generalisations are therefore only likely to be appropriate when n heavy signal particles are expected to be produced.

Our introduction focused on the simplest decay topologies of pair-produced heavy particles such as $\tilde{q}\tilde{q} \rightarrow q\tilde{\chi}_1^0 \bar{q}\tilde{\chi}_1^0$ but our simulations also show excellent discrimination in more complicated cases using the same m_{T_2} variable. Decay sequences with many steps, or indeed individual multi-daughter decays, such as $\tilde{g}\tilde{g} \rightarrow q\tilde{q}\tilde{\chi}_1^0 q\tilde{q}\tilde{\chi}_1^0$ (via three-body decays), could have been input to m_{T_2}

in a number of ways. There is no unique choice for constructing the two ‘visible particle systems’ from the ($k > 2$) decay products. We could have chosen to form two composite systems (two di-jet systems for the gluino example), and use these as the visible inputs to m_{T2} [7, 9]. This construction would have provided a large number of signal events close to the kinematic boundary and so would be appropriate for mass determination. However forming di-jet composite objects produces visible systems which no longer have $m_v \approx 0$, so one would lose the desirable properties of Lemmas 3, 5 – 7. For our search, even though cascade or multi-body decays are expected, we have still chosen to form $m_{T2}(j_1, j_2, \mathbf{p}_T, 0, 0)$ using *only* the two highest p_T jets — precisely as for the simpler di-jet topology. This way we retain the desirable properties (Lemmas 3, 5 – 7) for the backgrounds. The m_{T2} distribution for the signal can still extend up to large values (close to $m_{\tilde{g}}$ for the three-body decay), albeit with fewer near-maximal events than would be found by using composite two-jet visible systems. By inputting only the highest two p_T jets to m_{T2} , not only do we take advantage of the background rejection properties, but we also combine many signal channels together, forming a larger sample of signal events (which therefore enjoys a larger statistical significance).

Of course even having found a good discriminating variable one is not absolved from the need to understand the residual background contributions. Previous studies [6, 14] show that the rates of a wide variety of Standard Model processes can be measured in control regions using ⁷ It has recently been suggested that ISR jets could themselves provide a good indicator of mass scale [22].

the LHC collision data. These are then extrapolated to the signal region using techniques which themselves are validated by Monte Carlo simulation. Our m_{T2} signal region has a non-negligible contribution from vector boson production in association with two (or more) jets from initial state radiation. The dependence of such ISR jets on parameters such as \sqrt{s} and η is therefore of considerable interest; jets at large $|\eta|$ could, for example, provide an ISR-dominated control region.⁷ The fact that there is a large number of background events in the low m_{T2} region ($\lesssim m_t$) might actually turn out to be rather helpful – one can measure the total background contributions from this control region with high precision.

Complementary measurements will clearly be needed to disentangle the various background processes, so many observables will be used by the LHC experiments. Our analysis and simulations suggest that m_{T2} , the natural kinematic observable for pair-produced particles, ought to be at the front of the queue.

Acknowledgments

We are grateful to C.G. Lester and to B. Gripaios for encouraging the wider dissemination of these results, and to Mihoko Nojiri and the IPMU, Tokyo, Japan, for hosting the workshop which prompted those discussions. Further thanks to C.G. Lester, B. Gripaios and to A. Pinder, and K. Matchev for helpful comments and discussions. AJB and CG are supported by Advanced Fellowships from the UK Science and Technology Facilities Council.

-
- [1] G. Arnison et al. (UA1), Phys. Lett. **B122**, 103 (1983).
[2] J. J. Aubert et al. (E598), Phys. Rev. Lett. **33**, 1404 (1974); G. Arnison et al. (UA1), Phys. Lett. **B126**, 398 (1983); S. Abachi et al. (D0), Phys. Rev. Lett. **74**, 2632 (1995), hep-ex/9503003; F. Abe et al. (CDF), Phys. Rev. Lett. **74**, 2626 (1995), hep-ex/9503002.
[3] G. Arnison et al. (UA1), Phys. Lett. **B129**, 273 (1983); M. Banner et al. (UA2), Phys. Lett. **B122**, 476 (1983).
[4] S. Dimopoulos and H. Georgi, Nucl. Phys. **B193**, 150 (1981); H.-C. Cheng, K. T. Matchev, and M. Schmaltz, Phys. Rev. **D66**, 056006 (2002), hep-ph/0205314; H.-C. Cheng and I. Low, JHEP **09**, 051 (2003), hep-ph/0308199.
[5] C. G. Lester and D. J. Summers, Phys. Lett. **B463**, 99 (1999), hep-ph/9906349.
[6] G. Aad et al. (The ATLAS) (2009), 0901.0512.
[7] C. Lester and A. Barr, JHEP **12**, 102 (2007), 0708.1028; M. M. Nojiri, Y. Shimizu, S. Okada, and K. Kawagoe, JHEP **06**, 035 (2008), 0802.2412.
[8] H.-C. Cheng and Z. Han, JHEP **12**, 063 (2008), 0810.5178.
[9] W. S. Cho, K. Choi, Y. G. Kim, and C. B. Park, Phys. Rev. Lett. **100**, 171801 (2008), 0709.0288; A. J. Barr, B. Gripaios, and C. G. Lester, JHEP **02**, 014 (2008), 0711.4008.
[10] B. Gripaios, JHEP **02**, 053 (2008), 0709.2740; W. S. Cho, K. Choi, Y. G. Kim, and C. B. Park, JHEP **02**, 035 (2008), 0711.4526.
[11] B. C. Allanach, C. G. Lester, M. A. Parker, and B. R. Webber, JHEP **09**, 004 (2000), hep-ph/0007009; A. J. Barr, C. G. Lester, M. A. Parker, B. C. Allanach, and P. Richardson, JHEP **03**, 045 (2003), hep-ph/0208214; A. Barr, C. Lester, and P. Stephens, J. Phys. **G29**, 2343 (2003), hep-ph/0304226; G. Weiglein et al. (LHC/LC Study Group), Phys. Rept. **426**, 47 (2006), hep-ph/0410364; P. Meade and M. Reece, Phys. Rev. **D74**, 015010 (2006), hep-ph/0601124; M. Baumgart, T. Hartman, C. Kilic, and L.-T. Wang, JHEP **11**, 084 (2007), hep-ph/0608172; B. Fuks, AIP Conf. Proc. **903**, 165 (2007), hep-ph/0610316; W. S. Cho, Y. G. Kim, K. Y. Lee, C. B. Park, and Y. Shimizu, JHEP **04**, 054 (2007), hep-ph/0703163; J. P. Conlon, C. H. Kom, K. Suruliz, B. C. Allanach, and F. Quevedo, JHEP **08**, 061 (2007), 0704.3403; W. S. Cho and K. Choi, AIP Conf. Proc. **939**, 219 (2007), 0706.2871; H.-C. Cheng, J. F. Gunion, Z. Han, G. Marandella, and B. McElrath, JHEP **12**, 076 (2007), 0707.0030; B. Fuks (2007), 0710.2002; G. G. Ross and M. Serna, Phys. Lett. **B665**, 212 (2008), 0712.0943; M. M. Nojiri, G. Polesello, and D. R. Tovey, JHEP **05**, 014 (2008), 0712.2718; Y. No-

- mura, M. Papucci, and D. Stolarski, JHEP **07**, 055 (2008), 0802.2582; D. R. Tovey, JHEP **04**, 034 (2008), 0802.2879; M. M. Nojiri et al. (2008), 0802.3672; T. Han, R. Mahbubani, D. G. E. Walker, and L.-T. Wang, JHEP **05**, 117 (2009), 0803.3820; W. S. Cho, K. Choi, Y. G. Kim, and C. B. Park, Phys. Rev. **D78**, 034019 (2008), 0804.2185; M. Serna, JHEP **06**, 004 (2008), 0804.3344; K. Hamaguchi, E. Nakamura, and S. Shirai, Phys. Lett. **B666**, 57 (2008), 0805.2502; R. Kitano, JHEP **11**, 045 (2008), 0806.1057; A. J. Barr, G. G. Ross, and M. Serna, Phys. Rev. **D78**, 056006 (2008), 0806.3224; M. M. Nojiri, K. Sakurai, Y. Shimizu, and M. Takeuchi, JHEP **10**, 100 (2008), 0808.1094; S. Y. Choi, M. Drees, A. Freitas, and P. M. Zerwas, Phys. Rev. **D78**, 095007 (2008), 0808.2410; O. Brandt (ATLAS) (2008), 0808.2934; P. Wienemann (ATLAS), AIP Conf. Proc. **1078**, 286 (2009), 0809.2204; W. S. Cho, K. Choi, Y. G. Kim, and C. B. Park, Phys. Rev. **D79**, 031701 (2009), 0810.4853; M. Burns, K. Kong, K. T. Matchev, and M. Park, JHEP **03**, 143 (2009), 0810.5576; A. J. Barr, A. Pinder, and M. Serna, Phys. Rev. **D79**, 074005 (2009), 0811.2138; A. Read et al., J. Phys. Conf. Ser. **119**, 062041 (2008); P. Konar, K. Kong, and K. T. Matchev, JHEP **03**, 085 (2009), 0812.1042; J. Hisano, M. M. Nojiri, and W. Sreethawong, JHEP **06**, 044 (2009), 0812.4496; Y. Bai and Z. Han (2009), 0902.0006; M. Burns, K. T. Matchev, and M. Park, JHEP **05**, 094 (2009), 0903.4371; K. T. Matchev, F. Moortgat, L. Pape, and M. Park (2009), 0906.2417.
- [12] H. S. Lee (CDF) (2009), 0905.4659; *Simultaneous template-based top quark mass measurement in the lepton+jets and dilepton channels using 3.2 fb⁻¹ of CDF data (the dilepton channel uses a new variable mt₂)*, CDF note 9679.
- [13] A. Barr et al., in preparation.
- [14] *CMS physics technical design report, volume II* (2006), CERN-LHCC-2006-021, CMS-TDR-008-2.
- [15] M. Bähr et al. (2008), 0812.0529; M. Bähr et al. (2008), 0803.0883.
- [16] B. Allanach et al., Eur. Phys. J. **C25**, 113 (2002), hep-ph/0202233.
- [17] W. Porod, Comput. Phys. Commun. **153**, 275 (2003), hep-ph/0301101.
- [18] M. Cacciari and G. P. Salam, Phys. Lett. **B641**, 57 (2006), hep-ph/0512210.
- [19] M. Cacciari, G. P. Salam, and G. Soyez, JHEP **04**, 063 (2008), 0802.1189.
- [20] L. Randall and D. Tucker-Smith, Phys. Rev. Lett. **101**, 221803 (2008), 0806.1049.
- [21] (2008), CMS-PAS-SUS-08-005.
- [22] A. Papaefstathiou and B. Webber (2009), 0903.2013.